NANO LETTERS

pubs.acs.org/NanoLett Letter

Threshold Voltage Control through Solvent Doping of Monolayer MoS_2 Transistors

Kathryn Neilson,* Charles Mokhtarzadeh, Marc Jaikissoon, Robert K. A. Bennett, Pratyush Buragohain, Ashish Verma Penumatcha, Sai Siva Kumar Pinnepalli, Carly Rogan, Azimkhan Kozhakhmetov, Kirby Maxey, Scott Clendenning, Eric Pop, Matthew Metz, Uygar Avci, and Kevin P. O'Brien*

Cite This: *Nano Lett.* 2025, 25, 7778–7784 Read Online

ACCESS | Metrics & More | Article Recommendations | Supporting Information

ABSTRACT: Two-dimensional (2D) materials are promising for beyond-silicon logic due to their ultrathin bodies for atomically thin channels. A key challenge lies in doping, to enable high-performance devices with a predictable and tunable threshold voltage (V_T), while retaining switching behavior. In this work, we explore n-doping monolayer MoS_2 with solvents of varying polarity to both enhance transistor performance and understand how solvents impact the V_T. We find that solvent polarity predictably shifts the V_T when states are available near the MoS_2 conduction band. This n-doping shifts the V_T, increases the maximum on-current, and is achieved without significant degradation in the subthreshold swing. We also find that solvent doping reduces the Schottky barrier width, enabling a two-fold reduction in contact resistance. These findings provide a method to tune carrier concentrations by V_T shifting and offer clarity on the role solvents play in processing 2D devices.

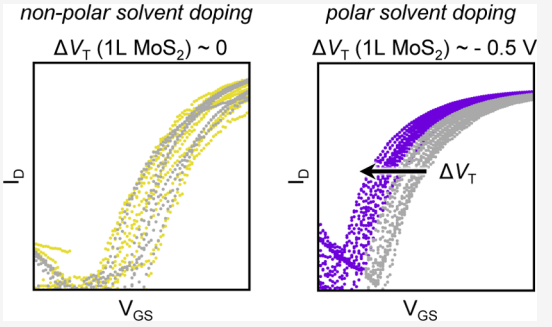

KEYWORDS: *two-dimensional (2D) materials, MoS_2, doping, threshold voltage*

The continued scaling of Moore's law requires novel solutions with regard to the device architecture and materials used in logic.[1] 2D semiconductors are attractive for future device technologies due to their relatively low temperature synthesis on arbitrary substrates,[2] enabling back-end-of-line processing and potential for stacked nanosheets. Their retained mobility in thin channels (compared to potential degradation in sub-2 nm thickness silicon[3,4]) is enabled by a van der Waals gap with no dangling bonds in the out-of-plane direction. Additionally, 2D semiconductors have retained electrostatic control at scaled gate lengths,[5] which make these materials attractive for beyond-Si channels in ultrascaled logic. However, in order to be implemented in high-volume manufacturing, 2D semiconductors (the most common of which are transition metal dichalcogenides, or TMDs) should have high on-currents,[6] low off-currents,[7] steep switching,[8] and a predictable threshold voltage (V_T) for circuit operation. While much work to date has been focused on increasing on-state current in 2D-based devices, few works to date claim "control" of the threshold voltage,[9] often adding a quantifiable, but difficult to tune, number of carriers to the system.[10−12]

One proposed doping method in 2D materials is charge transfer (i.e., modulation) doping (rather than substitutional), which can be achieved by either capping layers[13] or solvents[14,15] to shift the threshold voltage. Solvent doping has previously been demonstrated for n-type[14,16−19] and p-type[15,20] 2D semiconductors with a variety of solvents, all of which tune the carrier concentration. Additionally, throughout the device fabrication process, the use of solvents is inevitable through various cleaning and liftoff procedures;[17] therefore, it is advantageous to be able to predict the effect of solvents on the final device performance of a transistor. However, there exists a lack of understanding of the mechanism by which some, but not all, solvents dope 2D semiconductors.

In this work, we aim to both understand and predictably control the threshold voltage through exposing open-channel (i.e., uncapped) monolayer (1L) MoS_2 to solvents with a variety of polarities. We test seven solvents: steam, dimethyl sulfoxide (DMSO), pyridine, hexanes, dioxane, tetrahydrofuran (THF), and acetonitrile. These solvents encompass a range of relative polarities, from nonpolar to polar, and all tested solvents are reported. Additionally, we choose to measure the effect of solvents on unencapsulated devices, as common encapsulation layers tend to shift the threshold voltage[10,21] or are deposited using temperatures that may desorb the dopants

Received: February 3, 2025
Revised: April 15, 2025
Accepted: April 16, 2025
Published: May 2, 2025

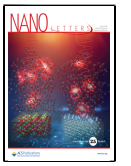

https://doi.org/10.1021/acs.nanolett.5c00734
Nano Lett. 2025, 25, 7778–7784

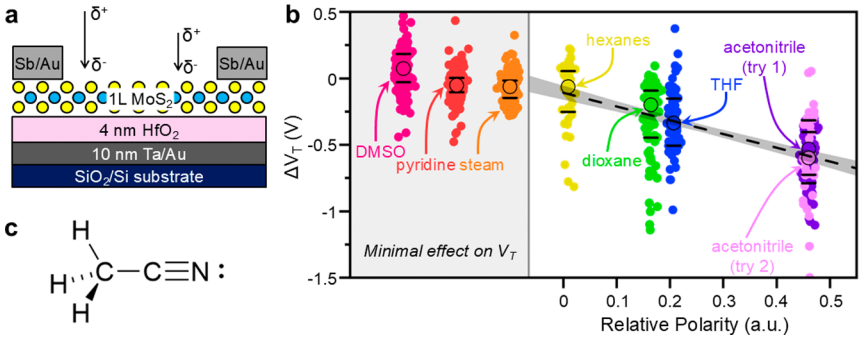

Figure 1. a, Schematic cross-section for monolayer MoS_2 devices used in this study. Channels are local back-gated with 4 nm of hafnia as a dielectric, Au as a metal gate, and contacted in the source/drain using Sb capped with Au. Devices are measured as-fabricated in N_2 ambient, then dipped for 60 seconds in a solvent, doping the device. **b**, Change in threshold voltage (ΔV_T) for solvent doping with varying polarities.[27] The left side of the figure shows those polar solvents that do not have an expected shift in the threshold voltage, including dimethyl sulfoxide (DMSO), pyridine, and steam. The right side of the figure shows those solvents that follow a trend with relative polarity of the solvent. Small circles are individual devices, large points outlined in black are the median, bars represent the first and third quartile of devices, and the gray fit line represents the 95% confidence interval. The change in V_T is calculated for the same device before and after doping. Acetonitrile was tested two separate times to check repeatability; try 1 and try 2 refer to the two attempts on separate samples, which subsequently show reproducibility. **c**, Schematic of acetonitrile.

(e.g., conventional atomic layer deposition[13]). Solvents that provide states near the conduction band of 1L MoS_2 show a temporary threshold voltage tunability (a decrease in V_T of ~210 mV per 0.1 increase in relative polarity for an EOT of ~1 nm) owing to dipoles created at the surface of the 2D semiconducting channel. This allows for reduced contact resistance due to the additional carriers near the source and drain, reducing the Schottky barrier width. Additionally, we show this doping with retained electrostatic control in the subthreshold regime, suggesting no additional surface scattering, and a retained transconductance. These results provide a tunable method to set the V_T and give further insight into how solvents affect 2D semiconductor devices.

To explore how solvent doping influences 2D semiconductors, we fabricated open-channel, local back-gated monolayer MoS_2 transistors (see the structure in Figure 1a). The fabrication is described in more detail in Methods. Each sample is first measured as-fabricated, then dipped for 60 s in each respective solvent, blown dry with N_2, and remeasured. Threshold voltage (V_T) changes (taken at a constant current of 1 nA μm^{-1}) from each solvent are reported for identical devices before and after doping. Solvents are chosen to span a wide range of polarities, from nonpolar to highly polar, to systematically test n-doping 1L MoS_2 versus polarity.

A Lewis base is a molecule with a filled nonbonding orbital capable of engaging in a dative bond with an unoccupied orbital on a Lewis acid to make a Lewis acid−base adduct. Accordingly, these interactions have been extensively documented within the organometallic chemistry literature, such that solvent coordination to metal atoms can modulate coordinative and/or electronic saturation, having a direct impact on the physical properties of the material.[22] While not all polar molecules function as a Lewis acid or base, those solvents that contain nonbonding lone pairs could physisorb to the TMD surface[23,24] and function as a charge donor to the system. While 2D materials are overall charge neutral, the polar covalent bonding between metal and chalcogenide atoms results in an uneven distribution of electron density.[25] This uneven charge distribution can allow for polar molecules to weakly physisorb (Figure S1a), although the exact location of physisorption will depend on the identity of the specific molecule[23] or the defect density.[26] Therefore, we expect polar molecules to weakly bind to the surface and shift the threshold voltage, subsequently doping the 2D material.

Comparing the threshold voltage (taken at a constant current of 1 nA/μm) of the same device before and after solvent exposure shows that the V_T shift is stronger with more polar solvents (Figure 1b). (Transfer characteristics for solvents shown in Figure 1b can be found in Figures S2−S7.) Approximately 2.5×10^{12} carriers/cm^2 are added per 100 mV of change in the threshold voltage (the carrier concentration is estimated by $n_{2D} = (C_{ox}/q)\cdot(V_{GS} - V_T)$ for small V_{DS}, where the threshold voltage is taken at a constant current of 1 nA/μm),[28] corresponding to a relative polarity increase of 0.08. Here, C_{ox} is the oxide capacitance per unit area, and q is the elementary charge. MoS_2 dipped in hexanes, a nonpolar molecule with poor Lewis basicity, shows an overall insignificant V_T shift, within typical variation. The dipole provided from a nonpolar solvent is expected to be small, as it is unlikely to physisorb to the MoS_2 surface or provide excess electrons for doping (Figure S1b); the small negative V_T shift may be due to a small amount of sample cleaning provided to the surface. Acetonitrile (Figure 1c), of comparatively large polarity, shows a large negative threshold voltage shift (~0.53 V) due to its larger dipole. This shift is repeatable; a solvent dip with a second sample (i.e., "try 2" shown in Figure 1b) leads to similar threshold voltage shifts. Dioxane and THF, with relative polarities and Lewis basicity between that of hexanes and acetonitrile, fall approximately within an expected linear trend of polarity versus threshold voltage shift, implying a predictive nature to solvent doping. However, because some solvents do not fall within the expected trend of V_T vs polarity, other factors are considered.

Despite the seemingly predictive nature with polarity and a subsequent dipole on the surface of MoS_2, not all polar solvents that adsorb onto the surface transfer charge to the 2D material. This phenomena has previously been observed in both graphene[29] and carbon nanotubes,[30] where otherwise polar molecules incorporated little to no charge transfer to the low-dimensional material. Solely the position of the lowest unoccupied molecular orbital (LUMO) and highest occupied molecular orbital (HOMO)[31] with respect to E_F and the MoS_2

https://doi.org/10.1021/acs.nanolett.5c00734
Nano Lett. 2025, 25, 7778−7784

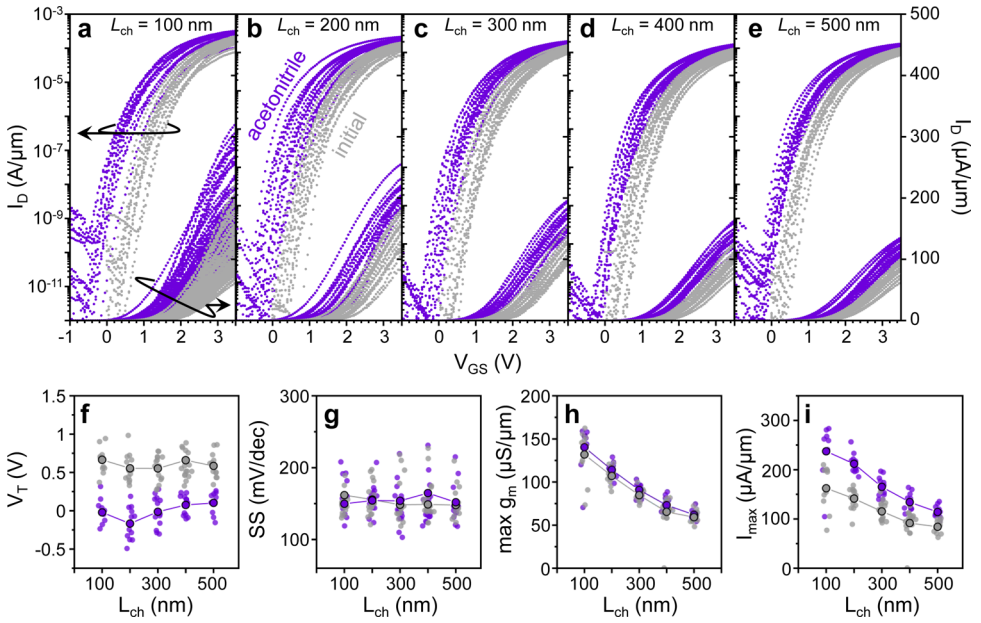

Figure 2. Device characteristics (~60 total) of monolayer MoS_2 before (gray) and after (purple) a 60 s dip in acetonitrile. Channel lengths range from **a**, 100 nm; **b**, 200 nm; **c**, 300 nm; **d**, 400 nm, to **e**, 500 nm and are shown in both log scale (left axis) and linear scale (right axis). An apparent negative shift in the threshold voltage is seen for all channel lengths, from initial (gray) to dipped in acetonitrile (purple). All transfer characteristics are shown for V_{DS} = 1 V. **f**, The threshold voltage (V_T) as a function of channel length, taken at a constant-current 1 nA/μm, before and after a solvent dip. A negative shift in the threshold voltage is seen for devices after solvent exposure. **g**, The subthreshold swing (SS), taken between 100 pA/μm and 1 nA/μm. No significant degradation of the SS is seen with doping, within typical variation. **h**, The maximum transconductance (g_m) before and after acetonitrile treatment. A minimal change is seen from the solvent, indicating that the transport properties of the 2D channel did not degrade. **i**, The maximum on-current (at max V_{GS}) before and after solvent treatment. The improvement in performance is slightly enhanced for shorter channels (100 nm) compared to long-channel (500 nm) devices. For all plots, symbols outlined in black are the averages for their respective device parameter. Only the forward sweep is shown for clarity.

conduction band are not sufficient to describe the doping behavior. Rather, on adsorption, solvents may provide a surface dipole with the 2D semiconductor, or the polar molecule can hybridize with the underlying material,[32] which may create states available for charge transfer. Depending on where these states lie with respect to the conduction and valence bands of the semiconductor, their magnitude with respect to E_F could then affect the doping magnitude. Therefore, any solvent expected to n-dope MoS_2 may interact such that states are present near the conduction band of MoS_2 in the solvent−semiconductor system; conversely, states may be present near the valence band for a p-dopant. DMSO, pyridine, and acetonitrile are all highly polar (relative polarities of 0.44, 0.302, and 0.46,[27] respectively), but do not transfer charge in the same manner as one another. Computational studies of acetonitrile adsorbed onto $PdSe_2$ report states ~0.5−1 eV above the Fermi level,[32] consistent with n-type doping. However, reports of DMSO adsorbed onto a 2D material calculate states present ~0.9 eV below E_F,[33] consistent with a small positive V_T shift, and reports of pyridine on metals are calculated to have no states at or above E_F upon adsorption to the surface,[34] consistent with no charge transfer.

To understand this solvent−2D interaction, the potential binding modes and the subsequent effect of the interface between the frontier molecular orbitals of the dopant and the relevant states from the 2D material must also be considered. For instance, although not a TMD surface, Turney *et al.*[35] showed that DMSO binds via the sulfur atom to Pt(111) surfaces (as opposed to an end-on coordination through the terminal oxygen).[35] Additionally, for pyridine it has been shown that a planar binding mode via the delocalized pi-system is preferential to end-on binding when absorbed onto Au(111)[36] and Si(111).[37] Both of these binding modes to a TMD surface could prevent the desired overlap of solvent and TMD orbitals, inhibiting sufficient charge transfer from the adsorbed molecule and the TMD surface.[29] Furthermore, the symmetry of the frontier orbitals and the orientation of the dopant must also be considered, such that proper overlap is achievable. It can thus be reasoned that THF, dioxane, and acetonitrile, by virtue of having localized lone pairs in the HOMO at the heteroatom in the solvent, demonstrate that the proper orbital symmetry, energy, and approach vector all play a key role in the ability to dope the TMD.[29] Further studies could aim to calculate the density of states of each solvent−semiconductor combination for varying solvent concentrations, molecular orientations, and adsorption locations to the semiconductor.

It should be noted that since the effectiveness of a dopant may depend on the orbital overlap and the location of the density of states with respect to the 2D material, solvents that may strongly dope 2D materials on one substrate may provide no V_T shift on another, as the band gap changes with layer count, and the substrate shifts both the conduction and valence bands of the 2D material.[38,39] Finally, steam (i.e., water), while highly polar, may not follow typical trends because of the dissociative nature of both hydrogen and hydroxyl groups, which can interact with MoS_2.[40] Water can then cause an unexpected counterclockwise hysteresis (Figure S8a).

Figure 2a−e show transfer characteristics of monolayer MoS_2 transistors before and after a 60 s dip in acetonitrile, the most effective n-dopant seen in this work (quantified in Figure 2f). Only the forward sweep is shown for clarity; typical

https://doi.org/10.1021/acs.nanolett.5c00734
Nano Lett. 2025, 25, 7778−7784

hysteresis is demonstrated in Figure S8b,c. Ideally, dopants will shift the V_T, while maintaining the transconductance (g_m) and the subthreshold swing (SS). In these devices, for a negative shift in the V_T (Figure 2f), little degradation in the SS (taken as the slope between 100 pA/μm and 1 nA/μm) is seen (Figure 2g); the device transconductances are retained (Figure 2h), and the on-state performance improves (Figure 2i). In this case, the combination of a comparatively short dip time (60 s) and a monolayer film may allow for retained electrostatic control as compared to previous works, which have shown that a significant amount of doping can cause the subthreshold to degrade.[14,16,19,41,42] Multilayer films tend to have a larger density of states than monolayers,[43] leading to a larger number of overall carriers in multilayer films, which could then degrade electrostatic control at high carrier concentrations. Additionally, band gap changes with layer count and dielectric environment[38] may further affect how solvents dope multilayer films.

In the on-state, an excess of carriers added to the system can increase carrier−carrier scattering and subsequently degrade the mobility of the channel, if the carrier concentration is high enough.[44] However, for the solvents presented herein, the electrostatic doping levels retain the mobility of the channel (when considering that the transconductance is proportional to mobility, as the exact mobility extraction may see inaccuracies[45−47]). It should be noted that the doping is not permanent (see Figure S9); after the time span of 1 week, the threshold voltage returns to a similar value to before the solvent treatment. Although the boiling point of these solvents is above room temperature, samples were stored for time-dependent studies in a desiccator, which likely desorbed the weakly physisorbed solvent on the surface.[23,48] Further studies may aim to make this doping more permanent by encapsulation (e.g., via low-temperature atomic layer deposition[49]) or higher adsorption energy solvents.

In addition to shifting the threshold voltage, the extra charge carriers provided from the solvent dopant also reduce the contact resistance (R_C) by up to 2×, from 3.2 k$\Omega\cdot\mu$m to 1.5 k$\Omega\cdot\mu$m (Figure 3a), fixed at a given carrier concentration (R_C, shown as a function of carrier concentration in Figure 3b). When a metal contacts a semiconductor, the metal can deplete the semiconductor of mobile carriers under the contact.[50] A problem arises in 2D semiconductors, where the contact depletion region may extend into the channel,[51] reducing the number of carriers at the contact edge. As the majority of carrier injection occurs near the contact edge in 2D semiconductors,[52] a decreased number of carriers results in a wider Schottky barrier, with an increased R_C. Adding dopants (in this case, from solvents, although it has been demonstrated previously with charge capping layers[10]) near injection at the contact provides additional charge to reduce the effective barrier width and subsequently reduce the contact resistance. The contact resistance is less dependent on the average carrier density (Figure 3b) compared to as-fabricated, suggesting the total resistance is more channel-dominant.

In summary, we have shown a predictable n-type doping of monolayer MoS_2 transistors. We find that solvent doping depends on the polarity of the molecule, which determines the amount of threshold voltage shift seen. However, the polarity alone is not sufficient to explain the solvent doping mechanism; the solvent−semiconductor system should also result in states above the Fermi level near the conduction band of MoS_2 or otherwise provide a dipole to n-dope the system.

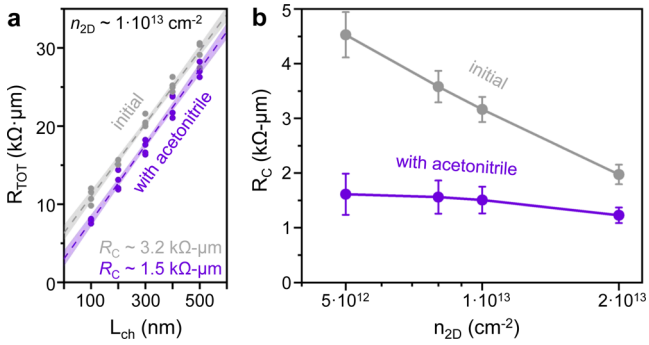

Figure 3. Contact resistance with and without doping from solvents. **a**, Contact resistance extraction using the transfer length method (TLM) before (gray) and after (purple) a dip in acetonitrile; total resistances (R_{TOT}) are extracted at a carrier density of ~10^{13} cm^{-2} for V_{DS} = 50 mV. The contact resistance is then extracted at the vertical intercept ($2R_C$), at L_{ch} = 0. Total resistance data points shown are from the best quartile of devices, and shaded regions represent the 95% confidence interval fit of the data. The TLM fit lines are parallel, suggesting constant mobility, which provides further evidence that the solvent does not degrade the channel properties. **b**, The contact resistance as a function of the carrier density, showing that the solvent doping allows for more constant R_c with carrier concentration, evidence that the contacts have a smaller Schottky barrier width than in an undoped case.

Using this knowledge, doping with a variety of solvents is shown to shift the threshold voltage with minimal degradation in both switching behavior and maximum transconductance while showing an increase in the on-current. Further, this doping increases the number of carriers in the otherwise depleted 2D semiconductor, reducing the contact resistance by decreasing the barrier width. This work helps explain the effect of solvents on 2D devices and provides a way to temporarily tune the threshold voltage in 2D transistors.

METHODS

Monolayer MoS_2 grown by molecular beam epitaxy is wet transferred onto Ta/Au (Ta interfacing with the SiO_2) local back gates with 4 nm of ALD HfO_2 serving as a back gate dielectric. The 2D material is etched using an ICP-RIE (inductively coupled plasma-reactive ion etching) reactor; subsequent channel widths range from 250 to 400 nm, dependent upon the specific sample. Electron-beam evaporated Sb/Au (10/20 nm) serves as the source and drain. Finally, metal pads are evaporated to probe the device. Each chip is first electrically measured (in N_2 ambient) before solvent treatment, then subsequently dipped and lightly agitated in its respective solvent for 60 seconds, blown dry with N_2, and then electrically measured immediately following the solvent treatment. Different samples are used for each solvent to reduce the effect of one solvent on another. Electrical measurements conclude within approximately 2 h of the solvent treatment. Note that no delamination of the channel is observed optically, as the channel is fixed to the substrate by the source and drain contacts. For stability measurements, samples are stored in a N_2 desiccator for 1 week and then re-measured.

ASSOCIATED CONTENT

Supporting Information

The Supporting Information is available free of charge at https://pubs.acs.org/doi/10.1021/acs.nanolett.5c00734.

https://doi.org/10.1021/acs.nanolett.5c00734
Nano Lett. 2025, 25, 7778−7784

Photoluminescence of MoS_2 before and after dips in acetonitrile and hexanes; transfer characteristics of MoS_2 after a 60 s dip in dimethyl sulfoxide, pyridine, steam, hexanes, dioxane, tetrahydrofuran; device hysteresis; stability of solvent doping after 1 week (PDF)

AUTHOR INFORMATION

Corresponding Authors

Kathryn Neilson − *Technology Research, Intel Corporation, Hillsboro, Oregon 97124, United States; Department of Electrical Engineering, Stanford University, Stanford, California 94305, United States;* orcid.org/0000-0003-1061-2919; Email: kmn@alumni.stanford.edu

Kevin P. O'Brien − *Technology Research, Intel Corporation, Hillsboro, Oregon 97124, United States;* Email: kevin.p.obrien@intel.com

Authors

Charles Mokhtarzadeh − *Technology Research, Intel Corporation, Hillsboro, Oregon 97124, United States*

Marc Jaikissoon − *Technology Research, Intel Corporation, Hillsboro, Oregon 97124, United States;* orcid.org/0000-0001-5102-6348

Robert K. A. Bennett − *Technology Research, Intel Corporation, Hillsboro, Oregon 97124, United States; Department of Electrical Engineering, Stanford University, Stanford, California 94305, United States;* orcid.org/0000-0001-7427-8724

Pratyush Buragohain − *Technology Research, Intel Corporation, Hillsboro, Oregon 97124, United States*

Ashish Verma Penumatcha − *Technology Research, Intel Corporation, Hillsboro, Oregon 97124, United States*

Sai Siva Kumar Pinnepalli − *Technology Research, Intel Corporation, Hillsboro, Oregon 97124, United States*

Carly Rogan − *Technology Research, Intel Corporation, Hillsboro, Oregon 97124, United States*

Azimkhan Kozhakhmetov − *Technology Research, Intel Corporation, Hillsboro, Oregon 97124, United States*

Kirby Maxey − *Technology Research, Intel Corporation, Hillsboro, Oregon 97124, United States*

Scott Clendenning − *Technology Research, Intel Corporation, Hillsboro, Oregon 97124, United States*

Eric Pop − *Department of Electrical Engineering, Department of Materials Science and Engineering, and Department of Applied Physics, Stanford University, Stanford, California 94305, United States;* orcid.org/0000-0003-0436-8534

Matthew Metz − *Technology Research, Intel Corporation, Hillsboro, Oregon 97124, United States*

Uygar Avci − *Technology Research, Intel Corporation, Hillsboro, Oregon 97124, United States*

Complete contact information is available at: https://pubs.acs.org/10.1021/acs.nanolett.5c00734

Notes

The authors declare no competing financial interest.

ACKNOWLEDGMENTS

K.N. and R.K.A.B. acknowledge support from the Stanford Graduate Fellowship (SGF), and K.N. would also like to acknowledge the National Science Foundation Graduate Research Fellowship Program (NSF-GRFP). K.N., R.K.A.B., and E.P. also acknowledge partial support from the Semiconductor Research Corporation (SRC) SUPREME Center.

REFERENCES

(1) Lundstrom, M. S.; Alam, M. A. Moore's law: The journey ahead. *Science* **2022**, *378* (6621), 722−723.

(2) Hoang, A. T.; Hu, L.; Kim, B. J.; Van, T. T. N.; Park, K. D.; Jeong, Y.; Lee, K.; Ji, S.; Hong, J.; Katiyar, A. K.; Shong, B.; Kim, K.; Im, S.; Chung, W. J.; Ahn, J.-H. Low-temperature growth of MoS_2 on polymer and thin glass substrates for flexible electronics. *Nat. Nanotechnol.* **2023**, *18* (12), 1439−1447.

(3) Uchida, K.; Junji, K.; Shin-ichi, T. In *Experimental study on carrier transport mechanisms in double- and single-gate ultrathin-body MOSFETs - Coulomb scattering, volume inversion, and dT_{SOI}−induced scattering*, IEEE International Electron Devices Meeting 2003, 8−10 Dec. 2003, 2003; pp 33.5.1−33.5.4.

(4) Agrawal, A.; Chakraborty, W.; Li, W.; Ryu, H.; Markman, B.; Hoon, S. H.; Paul, R. K.; Huang, C. Y.; Choi, S. M.; Rho, K.; Shu, A.; Iglesias, R.; Wallace, P.; Ghosh, S.; Cheong, K. L.; Hockel, J. L.; Thorman, R.; Baumgartel, L.; Shoer, L.; Mishra, V.; Berrada, S.; Ashita, A.; Weber, C.; Obradovic, B.; Oni, A. A.; Brooks, Z.; Franco, N.; Kavalieros, J.; Dewey, G. In *Silicon RibbonFET CMOS at 6nm Gate Length*, 2024 IEEE International Electron Devices Meeting (IEDM), 7−11 Dec. 2024, 2024; pp 1−4.

(5) O'Brien, K. P.; Naylor, C. H.; Dorow, C.; Maxey, K.; Penumatcha, A. V.; Vyatskikh, A.; Zhong, T.; Kitamura, A.; Lee, S.; Rogan, C.; Mortelmans, W.; Kavrik, M. S.; Steinhardt, R.; Buragohain, P.; Dutta, S.; Tronic, T.; Clendenning, S.; Fischer, P.; Putna, E. S.; Radosavljevic, M.; Metz, M.; Avci, U. Process integration and future outlook of 2D transistors. *Nat. Commun.* **2023**, *14* (1), 6400.

(6) Li, W.; Gong, X.; Yu, Z.; Ma, L.; Sun, W.; Gao, S.; Köroğlu, Ç.; Wang, W.; Liu, L.; Li, T.; Ning, H.; Fan, D.; Xu, Y.; Tu, X.; Xu, T.; Sun, L.; Wang, W.; Lu, J.; Ni, Z.; Li, J.; Duan, X.; Wang, P.; Nie, Y.; Qiu, H.; Shi, Y.; Pop, E.; Wang, J.; Wang, X. Approaching the quantum limit in two-dimensional semiconductor contacts. *Nature* **2023**, *613* (7943), 274−279.

(7) Kshirsagar, C. U.; Xu, W.; Su, Y.; Robbins, M. C.; Kim, C. H.; Koester, S. J. Dynamic Memory Cells Using MoS_2 Field-Effect Transistors Demonstrating Femtoampere Leakage Currents. *ACS Nano* **2016**, *10* (9), 8457−8464.

(8) Lan, H. Y.; Tripathi, R.; Appenzeller, J.; Chen, Z. Near-Ideal Subthreshold Swing in Scaled 2D Transistors: The Critical Role of Monolayer hBN Passivation. *IEEE Electron Device Letters* **2024**, *45* (7), 1337−1340.

(9) Ko, J. S.; Shearer, A. B.; Lee, S.; Neilson, K.; Jaikissoon, M.; Kim, K.; Bent, S. F.; Pop, E.; Saraswat, K. C. Achieving 1-nm-Scale Equivalent Oxide Thickness Top-Gate Dielectric on Monolayer Transition Metal Dichalcogenide Transistors With CMOS-Friendly Approaches. *IEEE Transactions on Electron Devices* **2025**, *72* (3), 1514−1519.

(10) Cai, L.; McClellan, C. J.; Koh, A. L.; Li, H.; Yalon, E.; Pop, E.; Zheng, X. Rapid Flame Synthesis of Atomically Thin MoO_3 down to Monolayer Thickness for Effective Hole Doping of WSe_2. *Nano Lett.* **2017**, *17* (6), 3854−3861.

(11) Wang, Z.; Tripathi, M.; Golsanamlou, Z.; Kumari, P.; Lovarelli, G.; Mazziotti, F.; Logoteta, D.; Fiori, G.; Sementa, L.; Marega, G. M.; Ji, H. G.; Zhao, Y.; Radenovic, A.; Iannaccone, G.; Fortunelli, A.; Kis, A. Substitutional p-Type Doping in NbS_2−MoS_2 Lateral Heterostructures Grown by MOCVD. *Advanced Materials* **2023**, *35* (14), No. 2209371.

(12) Kozhakhmetov, A.; Schuler, B.; Tan, A. M. Z.; Cochrane, K. A.; Nasr, J. R.; El-Sherif, H.; Bansal, A.; Vera, A.; Bojan, V.; Redwing, J. M.; Bassim, N.; Das, S.; Hennig, R. G.; Weber-Bargioni, A.; Robinson, J. A. Scalable Substitutional Re-Doping and its Impact on the Optical and Electronic Properties of Tungsten Diselenide. *Advanced Materials* **2020**, *32* (50), No. 2005159.

(13) McClellan, C. J.; Yalon, E.; Smithe, K. K. H.; Suryavanshi, S. V.; Pop, E. High Current Density in Monolayer MoS_2 Doped by AlO_x. *ACS Nano* **2021**, *15* (1), 1587−1596.

(14) Li, X.-K.; Sun, R.-X.; Guo, H.-W.; Su, B.-W.; Li, D.-K.; Yan, X.-Q.; Liu, Z.-B.; Tian, J.-G. Controllable Doping of Transition-Metal Dichalcogenides by Organic Solvents. *Advanced Electronic Materials* **2020**, *6* (3), No. 1901230.
(15) Kang, D.-H.; Shim, J.; Jang, S. K.; Jeon, J.; Jeon, M. H.; Yeom, G. Y.; Jung, W.-S.; Jang, Y. H.; Lee, S.; Park, J.-H. Controllable Nondegenerate p-Type Doping of Tungsten Diselenide by Octadecyltrichlorosilane. *ACS Nano* **2015**, *9* (2), 1099−1107.
(16) Kiriya, D.; Tosun, M.; Zhao, P.; Kang, J. S.; Javey, A. Air-Stable Surface Charge Transfer Doping of MoS_2 by Benzyl Viologen. *J. Am. Chem. Soc.* **2014**, *136* (22), 7853−7856.
(17) Poddar, P. K.; Zhong, Y.; Mannix, A. J.; Mujid, F.; Yu, J.; Liang, C.; Kang, J.-H.; Lee, M.; Xie, S.; Park, J. Resist-Free Lithography for Monolayer Transition Metal Dichalcogenides. *Nano Lett.* **2022**, *22* (2), 726−732.
(18) Choi, J.; Zhang, H.; Du, H.; Choi, J. H. Understanding Solvent Effects on the Properties of Two-Dimensional Transition Metal Dichalcogenides. *ACS Appl. Mater. Interfaces* **2016**, *8* (14), 8864−8869.
(19) Yarali, M.; Zhong, Y.; Reed, S. N.; Wang, J.; Ulman, K. A.; Charboneau, D. J.; Curley, J. B.; Hynek, D. J.; Pondick, J. V.; Yazdani, S.; Hazari, N.; Quek, S. Y.; Wang, H.; Cha, J. J. Near-Unity Molecular Doping Efficiency in Monolayer MoS_2. *Advanced Electronic Materials* **2021**, *7* (2), No. 2000873.
(20) Li, Z.; Li, D.; Wang, H.; Xu, X.; Pi, L.; Chen, P.; Zhai, T.; Zhou, X. Universal p-Type Doping via Lewis Acid for 2D Transition-Metal Dichalcogenides. *ACS Nano* **2022**, *16* (3), 4884−4891.
(21) Ko, J. S.; Shearer, A.; Lee, S.; Neilson, K.; Jaikissoon, M.; Kim, K.; Bent, S.; Saraswat, K.; Pop, E. In *Achieving 1-nm-Scale Equivalent Oxide Thickness Top Gate Dielectric on Monolayer Transition Metal Dichalcogenide Transistors with CMOS-Friendly Approaches*, 2024 IEEE Symposium on VLSI Technology and Circuits (VLSI Technology and Circuits), 16−20 June 2024, 2024; pp 1−2.
(22) Gutmann, V. Solvent effects on the reactivities of organometallic compounds. *Coordination Chemistry Reviews* **1976**, *18* (2), 225−255.
(23) Patil, U.; Caffrey, N. M. Adsorption of common solvent molecules on graphene and MoS_2 from first-principles. *J. Chem. Phys.* **2018**, *149* (9), No. 094702.
(24) Brkić, A. L.; Supina, A.; Čapeta, D.; Dončević, L.; Ptiček, L.; Mandić, Š.; Racané, L.; Delač, I., Influence of Solvents and Adsorption of Organic Molecules on the Properties of CVD Synthesized 2D MoS_2. *Nanomaterials* **2023**, *13*, 2115.
(25) López-Galán, O. A.; Ramos, M.; Nogan, J.; Ávila-García, A.; Boll, T.; Heilmaier, M. The electronic states of ITO−MoS_2: Experiment and theory. *MRS Commun.* **2022**, *12* (2), 137−144.
(26) Bobbitt, N. S.; Chandross, M. Interactions of Water with Pristine and Defective MoS_2. *Langmuir* **2022**, *38* (34), 10419−10429.
(27) Reichardt, C.; Welton, T. Empirical Parameters of Solvent Polarity. *In Solvents and Solvent Effects in Organic Chemistry* **2010**, 425−508.
(28) Radisavljevic, B.; Kis, A. Mobility engineering and a metal−insulator transition in monolayer MoS_2. *Nature Materials* **2013**, *12* (9), 815−820.
(29) Leenaerts, O.; Partoens, B.; Peeters, F. M. Adsorption of H_2O, NH_3, CO, NO_2, and NO on graphene: A first-principles study. *Phys. Rev. B* **2008**, *77* (12), No. 125416.
(30) Zambano, A. J.; Talapatra, S.; Lafdi, K.; Aziz, M. T.; McMillin, W.; Shaughnessy, G.; Migone, A. D.; Yudasaka, M.; Iijima, S.; Kokai, F.; Takahashi, K. Adsorbate binding energy and adsorption capacity of xenon on carbon nanohorns. *Nanotechnology* **2002**, *13* (2), 201.
(31) Liu, H.; Wang, Y.; Mo, W.; Tang, H.; Cheng, Z.; Chen, Y.; Zhang, S.; Ma, H.; Li, B.; Li, X. Dendrimer-Based, High-Luminescence Conjugated Microporous Polymer Films for Highly Sensitive and Selective Volatile Organic Compound Sensor Arrays. *Adv. Funct. Mater.* **2020**, *30* (13), No. 1910275.
(32) Tien, N. T.; Dang, N. H.; Bich Thao, P. T.; Vo, K. D.; Hoat, D. M.; Nguyen, D. K. Adsorption effects of acetone and acetonitrile on defected penta-$PdSe_2$ nanoribbons: a DFT study. *RSC Adv.* **2024**, *14* (23), 16445−16458.
(33) Fernández-Escamilla, H. N.; Guerrero-Sánchez, J.; Garcia-Diaz, R.; Martínez-Guerra, E.; Takeuchi, N. Adsorption of dimethyl sulfoxide on blue phosphorene. *Surface Science* **2019**, *680*, 88−94.
(34) Benbella, A.; Matrane, I.; Badawi, M.; Lebègue, S.; Mazroui, M. A density functional theory study of thiophene and pyridine adsorption on Pt/Rh-doped Cu (100) surface. *Surface Science* **2023**, *729*, No. 122212.
(35) Sexton, B. A.; Avery, N. R.; Turney, T. W. A spectroscopic study of the coordination of dimethyl sulfoxide to a platinum (111) surface. *Surface Science* **1983**, *124* (1), 162−174.
(36) Mollenhauer, D.; Gaston, N.; Voloshina, E.; Paulus, B. Interaction of Pyridine Derivatives with a Gold (111) Surface as a Model for Adsorption to Large Nanoparticles. *J. Phys. Chem. C* **2013**, *117* (9), 4470−4479.
(37) Zhang, Y. P.; Wang, S.; Xu, G. Q.; Tok, E. S. Tuning Molecular Binding Configurations of Pyridine on Si(111)-(7×7) via Surface Modification. *J. Phys. Chem. C* **2011**, *115* (5), 2140−2145.
(38) Ryou, J.; Kim, Y.-S.; Kc, S.; Cho, K. Monolayer MoS_2 Bandgap Modulation by Dielectric Environments and Tunable Bandgap Transistors. *Sci. Rep.* **2016**, *6* (1), No. 29184.
(39) Mak, K. F.; Lee, C.; Hone, J.; Shan, J.; Heinz, T. F. Atomically Thin MoS_2: A New Direct-Gap Semiconductor. *Physical Review Letters* **2010**, *105* (13), No. 136805.
(40) Abidi, N.; Bonduelle-Skrzypczak, A.; Steinmann, S. N. Revisiting the Active Sites at the MoS_2/H_2O Interface via Grand-Canonical DFT: The Role of Water Dissociation. *ACS Appl. Mater. Interfaces* **2020**, *12* (28), 31401−31410.
(41) Zhao, P.; Kiriya, D.; Azcatl, A.; Zhang, C.; Tosun, M.; Liu, Y.-S.; Hettick, M.; Kang, J. S.; McDonnell, S.; Kc, S.; Guo, J.; Cho, K.; Wallace, R. M.; Javey, A. Air Stable p-Doping of WSe_2 by Covalent Functionalization. *ACS Nano* **2014**, *8* (10), 10808−10814.
(42) Kim, I.; Higashitarumizu, N.; Rahman, I. K. M. R.; Wang, S.; Kim, H. M.; Geng, J.; Prabhakar, R. R.; Ager, J. W., III; Javey, A. Low Contact Resistance WSe_2 p-Type Transistors with Highly Stable, CMOS-Compatible Dopants. *Nano Lett.* **2024**, *24* (43), 13528−13533.
(43) Wang, K.-C.; Stanev, T. K.; Valencia, D.; Charles, J.; Henning, A.; Sangwan, V. K.; Lahiri, A.; Mejia, D.; Sarangapani, P.; Povolotskyi, M.; Afzalian, A.; Maassen, J.; Klimeck, G.; Hersam, M. C.; Lauhon, L. J.; Stern, N. P.; Kubis, T. Control of interlayer physics in 2H transition metal dichalcogenides. *Journal of Applied Physics* **2017**, *122* (22), No. 224302.
(44) Thurber, W. R.; Mattis, R. L.; Liu, Y. M.; Filliben, J. J. Resistivity-Dopant Density Relationship for Phosphorus-Doped Silicon. *J. Electrochem. Soc.* **1980**, *127* (8), 1807.
(45) Nasr, J. R.; Schulman, D. S.; Sebastian, A.; Horn, M. W.; Das, S. Mobility Deception in Nanoscale Transistors: An Untold Contact Story. *Advanced Materials* **2019**, *31* (2), No. 1806020.
(46) Wu, P. Mobility overestimation in molybdenum disulfide transistors due to invasive voltage probes. *Nature Electronics* **2023**, *6* (11), 836−838.
(47) Bennett, R. K. A.; Hoang, L.; Cremers, C.; Mannix, A. J.; Pop, E. Mobility and threshold voltage extraction in transistors with gate-voltage-dependent contact resistance. *npj 2D Materials and Applications* **2025**, *9* (1), 13.
(48) Zhao, S.; Xue, J.; Kang, W. Gas adsorption on MoS_2 monolayer from first-principles calculations. *Chemical Physics Letters* **2014**, *595-596*, 35−42.
(49) Zhang, Z.; Passlack, M.; Pitner, G.; Kuo, C.-H.; Ueda, S. T.; Huang, J.; Kashyap, H.; Wang, V.; Spiegelman, J.; Lam, K.-T.; Liang, Y.-C.; Liew, S. L.; Hsu, C.-F.; Kummel, A. C.; Bandaru, P. Sub-Nanometer Interfacial Oxides on Highly Oriented Pyrolytic Graphite and Carbon Nanotubes Enabled by Lateral Oxide Growth. *ACS Appl. Mater. Interfaces* **2022**, *14* (9), 11873−11882.
(50) Szabó, Á.; Jain, A.; Parzefall, M.; Novotny, L.; Luisier, M. Electron Transport through Metal/MoS_2 Interfaces: Edge- or Area-Dependent Process? *Nano Lett.* **2019**, *19* (6), 3641−3647.

https://doi.org/10.1021/acs.nanolett.5c00734
Nano Lett. 2025, 25, 7778−7784

(51) Zhang, P.; Zhang, Y.; Wei, Y.; Jiang, H.; Wang, X.; Gong, Y. Contact engineering for two-dimensional semiconductors. *Journal of Semiconductors* **2020**, *41* (7), No. 071901.
(52) Arutchelvan, G.; Lockhart de la Rosa, C. J.; Matagne, P.; Sutar, S.; Radu, I.; Huyghebaert, C.; De Gendt, S.; Heyns, M. From the metal to the channel: a study of carrier injection through the metal/2D MoS_2 interface. *Nanoscale* **2017**, *9* (30), 10869−10879.

https://doi.org/10.1021/acs.nanolett.5c00734
Nano Lett. 2025, 25, 7778−7784

Supporting Information

Threshold Voltage Control through Solvent Doping of Monolayer MoS_2 Transistors

Kathryn Neilson[1,2*], Charles Mokhtarzadeh[1], Marc Jaikissoon[1], Robert K. A. Bennett[1,2], Pratyush Buragohain[1], Ashish Verma Penumatcha[1], Sai Siva Kumar Pinnepalli[1], Carly Rogan[1], Azimkhan Kozhakhmetov[1], Kirby Maxey[1], Scott Clendenning[1], Eric Pop[2,3,4], Matthew Metz[1], Uygar Avci[1] and Kevin P. O'Brien[1*]

[1] *Technology Research, Intel Corporation, Hillsboro, OR 97124*
[2] *Department of Electrical Engineering, Stanford University, Stanford, CA 94305*
[3] *Department of Materials Science and Engineering, Stanford University, Stanford, CA 94305*
[4] *Department of Applied Physics, Stanford University, Stanford, CA 94305*

*Corresponding Author: kmn@alumni.stanford.edu, kevin.p.obrien@intel.com

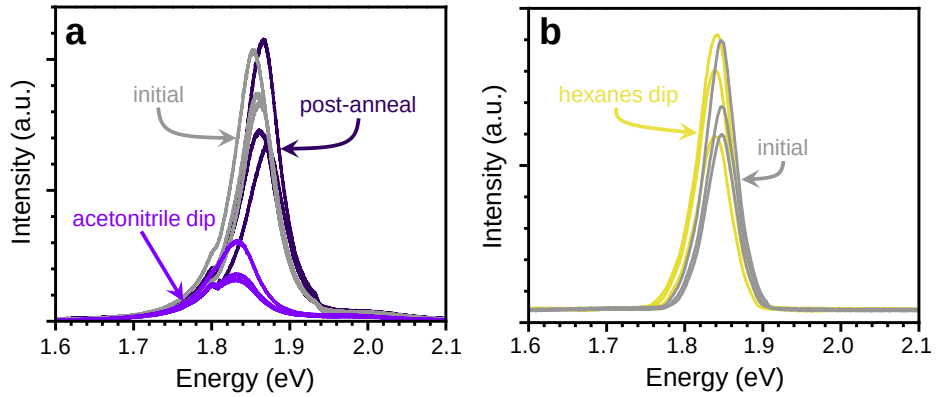

Figure S1: Photoluminescence (PL) of 1L CVD (chemical vapor deposition) MoS_2. **a,** PL of as-synthesized MoS_2 (grey), followed by a 60 s dip in acetonitrile (light purple), and finally after a 60 s hot plate anneal in ambient at 92 °C (dark purple). The acetonitrile shifts the 1L MoS_2 emission to a lower energy, suggesting increased charged exciton (trion) emissions from doping, as seen in previous work.[1] After an anneal above the boiling point of the solvent, the PL returns to approximately the as-synthesized peak position, suggesting the solvents could be physiosorbed to the 2D semiconductor. **b,** Photoluminescence of as-synthesized (grey) and after a 60s dip in hexanes (yellow) of 1L MoS_2. No significant change in the optical spectra is seen, which is consistent with the minimal V_T shift shown in **Figure 1b**, implying minimal doping. For all conditions, different spectra represent different grains of MoS_2. Here, λ = 532 nm.

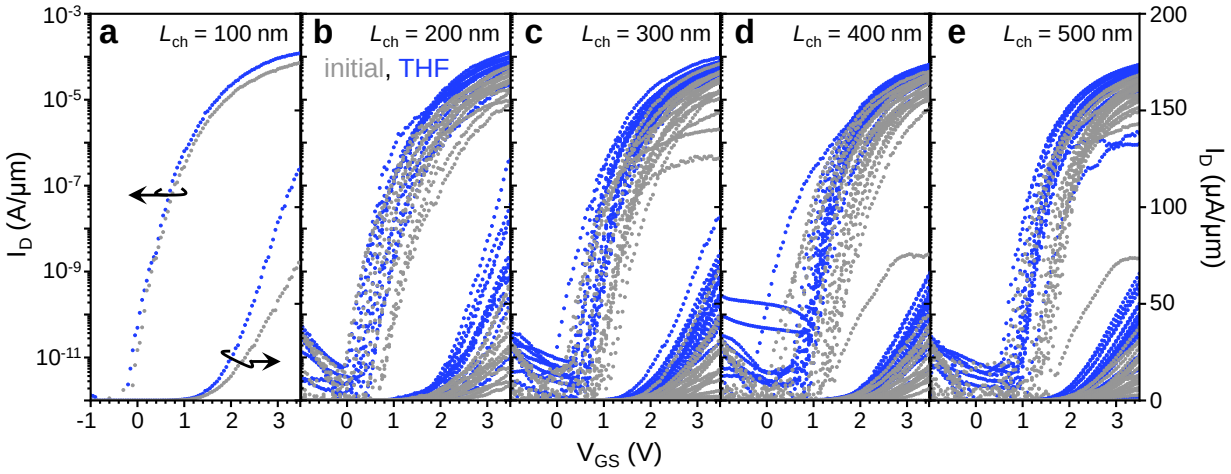

Figure S2: Transfer characteristics for multiple devices before (grey) and after (blue) solvent treatment in tetrahydrofuran (THF). **a-e** represents channel lengths from 100 nm to 500 nm, respectively. All devices are measured at V_{DS} = 1 V.

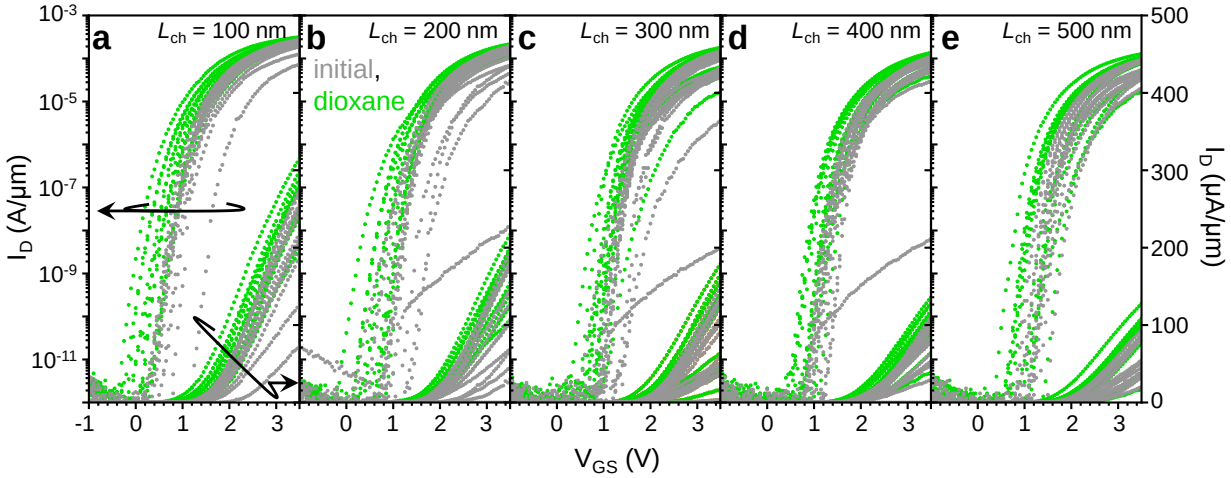

Figure S3: Transfer characteristics for multiple devices before (grey) and after (green) a solvent treatment in dioxane. **a-e** represents channel lengths from 100 nm to 500 nm, respectively. All devices are measured at V_{DS} = 1 V.

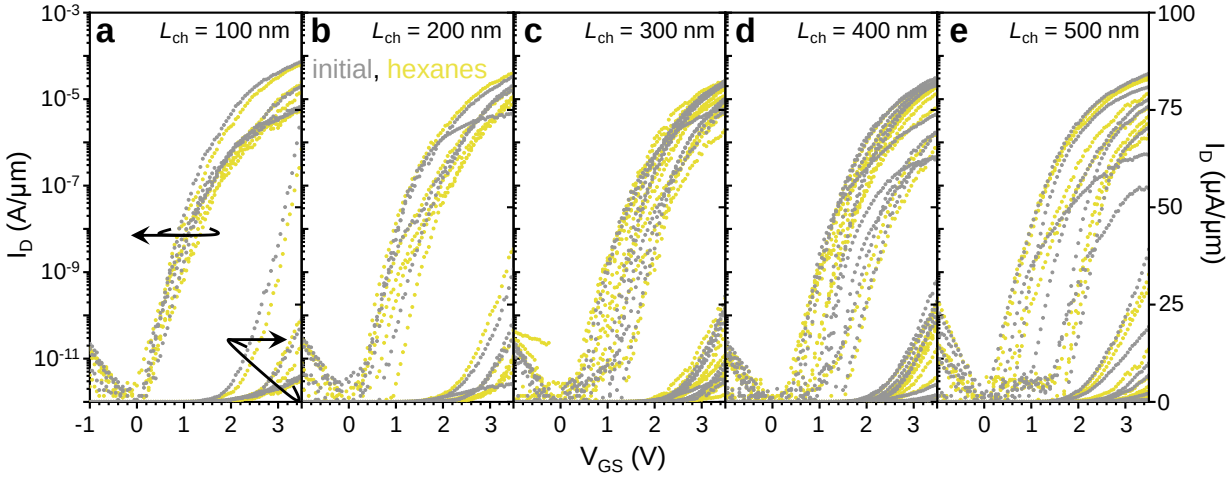

Figure S4: Transfer characteristics for multiple devices before (grey) and after (yellow) a solvent treatment in hexanes. **a-e** represents channel lengths from 100 nm to 500 nm, respectively. All devices are measured at V_{DS} = 1 V.

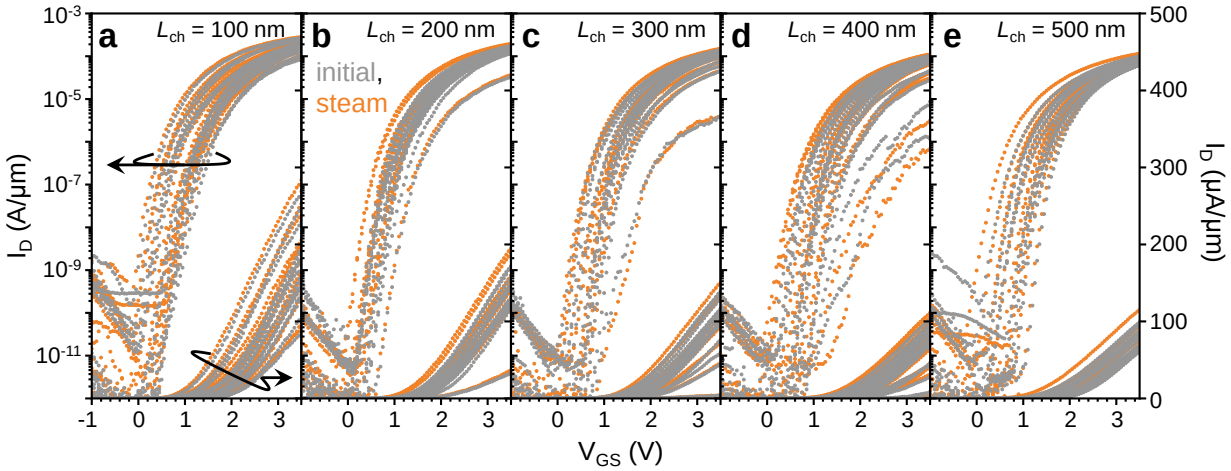

Figure S5: Transfer characteristics for multiple devices before (grey) and after (orange) a treatment in steam. **a-e** represents channel lengths from 100 nm to 500 nm, respectively. All devices are measured at V_{DS} = 1 V.

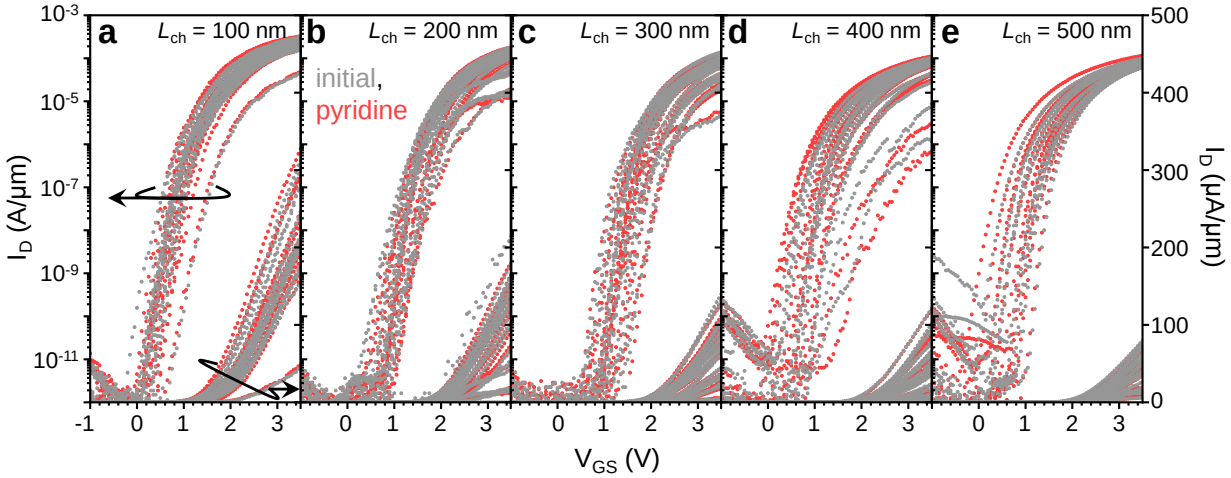

Figure S6: Transfer characteristics for multiple devices before (grey) and after (red) a solvent treatment in pyridine. **a-e** represents channel lengths from 100 nm to 500 nm, respectively. All devices are measured at V_{DS} = 1 V.

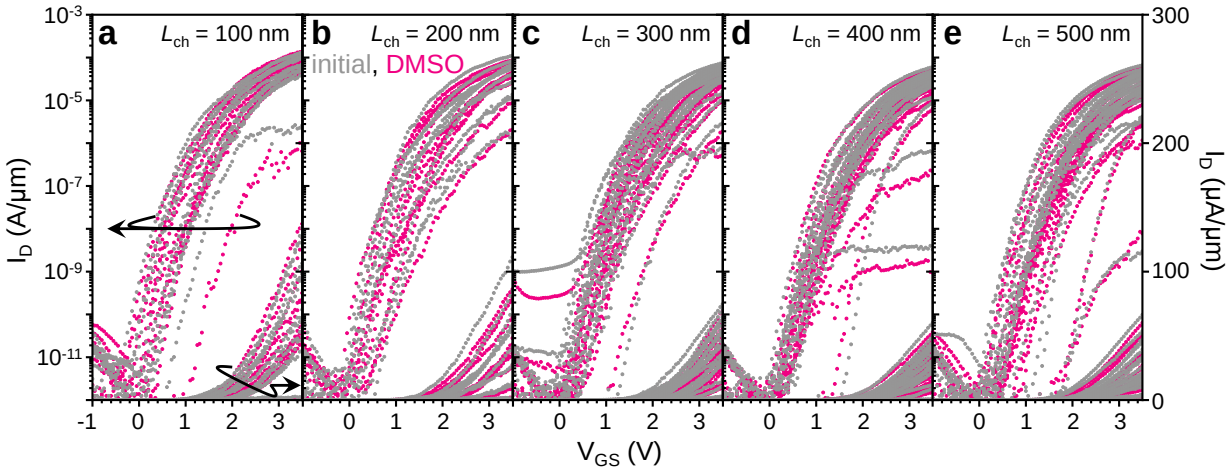

Figure S7: Transfer characteristics for multiple devices before (grey) and after (pink) a solvent treatment in dimethyl sulfoxide (DMSO). **a-e** represents channel lengths from 100 nm to 500 nm, respectively. All devices are measured at V_{DS} = 1 V.

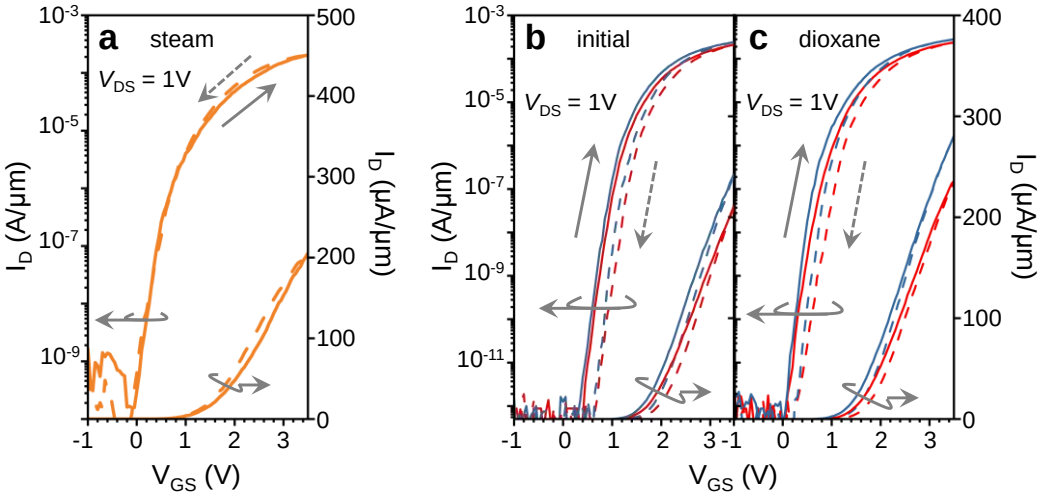

Figure S8: **a,** A device after exposure to steam. The hysteresis switches directions and becomes counterclockwise (rather than the typical clockwise) in the on-state. The channel length is 100 nm. **b,** Initial measurement of typical monolayer MoS_2 devices. Red and blue represent two different devices, solid lines represent the forward sweep, and dashed lines represent the reverse sweep. The channel length in both devices is 100 nm. **c,** The same devices measured after a solvent dip in dioxane. Little change in hysteresis is seen after these solvent dips.

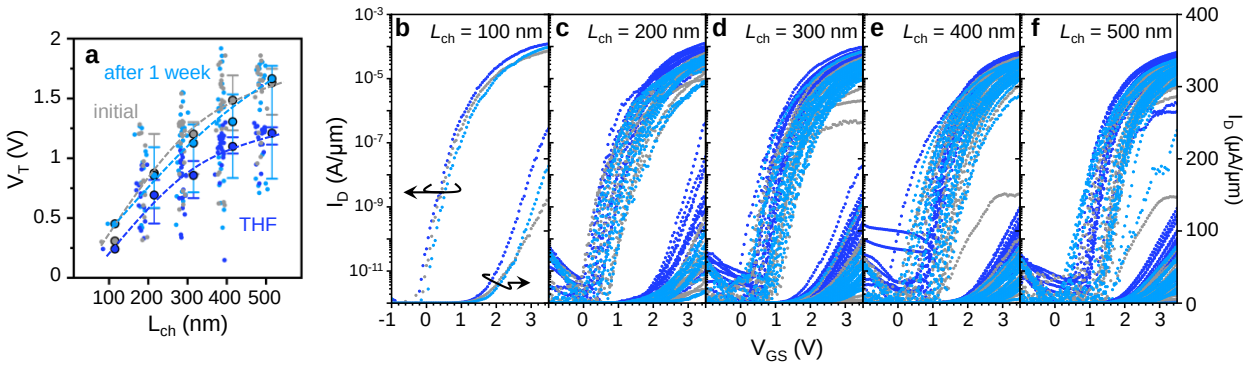

Figure S9: a, The forward-sweep constant current threshold voltage taken at 1 nA/μm. The grey symbols indicate the initial measurement, dark blue immediately following a dip in tetrahydrofuran (THF), and light blue after 1 week of storage in a nitrogen desiccator. The threshold voltage shifts more positive over time, reducing the effectiveness of solvent doping. **b,** Transfer characteristics showing stability of 100 nm, **c,** 200 nm, **d,** 300 nm **e,** 400 nm, and **e,** 500 nm channels. Grey points represent the initial device measurements, dark blue represent after a 60 s dip in THF, and light blue are after 1 week in a nitrogen desiccator. Devices return to similar operation (the initial measurement) after 1 week in a desiccator. All devices are measured at V_{DS} = 1 V.

References

1. Choi, J.; Zhang, H.; Du, H.; Choi, J. H., Understanding Solvent Effects on the Properties of Two-Dimensional Transition Metal Dichalcogenides. *ACS Applied Materials & Interfaces* **2016,** *8* (14), 8864-8869.